

High-pressure transitions to a postcotunnite phase in ionic AX_2 compounds

J. M. Léger, J. Haines, and A. Atouf

Centre National de la Recherche Scientifique, Laboratoire de Physico-Chimie des Matériaux,
1, Place Aristide Briand, 92190 Meudon, France

(Received 16 August 1994; revised manuscript received 14 October 1994)

The highest coordination known in ionic AX_2 compounds is found in the orthorhombic cotunnite ($PbCl_2$) structure, in which the metal ion is in ninefold coordination. Four cotunnite-structured compounds, $PbCl_2$, $BaCl_2$, $BaBr_2$, and $SnCl_2$, were investigated under high pressure by x-ray diffraction and were found to undergo phase transitions to the same postcotunnite phase at pressures between 7 and 16 GPa. The high-pressure phase is monoclinic, of space group $P112_1/a$, $Z=8$, with a structure in which the metal coordination number is ten, a value which up to the present has only been observed for covalent and metallic AB_2 compounds. This postcotunnite structure observed here is of considerable importance for the crystal chemistry of the AX_2 compounds as under ambient conditions over 400 compounds are isostructural to $PbCl_2$ and many others transform to a cotunnite structure at high pressures, which up to the present was the final known step in the phase-transition sequence of these materials. This new phase is $4.5 \pm 0.5\%$ denser than the cotunnite type in the *csae* of $PbCl_2$ at 16 GPa.

I. INTRODUCTION

Under ambient conditions the cotunnite ($PbCl_2$) structure is the example of the highest known coordination in ionic AX_2 compounds, which include many important minerals, such as SiO_2 . This cotunnite structure represents the final known step in the phase-transition sequence of the AX_2 compounds investigated to date.

The structures of the AX_2 compounds can be divided in four main groups based upon the constituent cation-centered anion polyhedra: the quartz group, the rutile group, the fluorite group, and the cotunnite group, in which the metal coordination number (CN) is four (tetrahedron), six (octahedron), eight (cube), and nine (elongated tricapped trigonal prism), respectively. Many

distorted variants of these basic structures exist as do many layer structures, which can be related to one of these main structure types. Under ambient conditions, over 400 compounds adopt the orthorhombic cotunnite structure,¹ space group $Pnam$, $Z=4$, Fig. 1.

Under high pressure, numerous phase transitions occur in the AX_2 compounds,² at which, in many cases, there is an increase in coordination number of the metal ion. These increases in coordination number result from an increase in the cation-anion radius ratio, r_c/r_a , due to the greater relative compressibility of anions. In SiO_2 at high pressure, coesite transforms to stishovite corresponding to an increase in the silicon coordination number from four to six.³ Similarly, an increase in the Pb^{4+} CN from 6 to 8 and subsequently to 9 occurs when rutile-structured

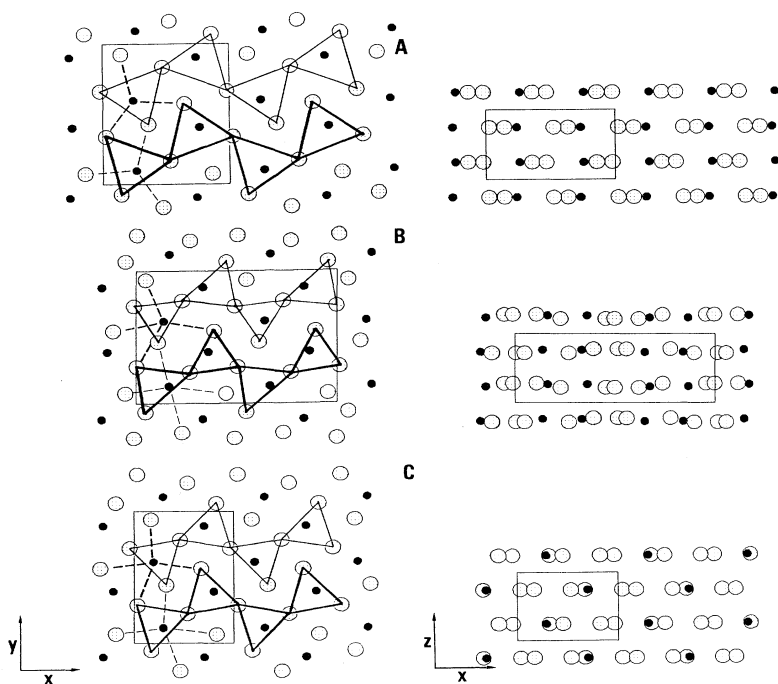


FIG. 1. Projections of the structures of cotunnite $PbCl_2$ at ambient pressure (A), postcotunnite $PbCl_2$ at 25.4 GPa (B) and a hypothetical Co_2Si -type $PbCl_2$ (C) in the xy and xz planes. Small and large circles represent Pb^{2+} and Cl^- , respectively. The unit cells are outlined. Trigonal prisms with cations at z and $z + \frac{1}{2}$ are represented by thick and thin solid lines, respectively; dashed lines indicate the remaining anions in the coordination sphere for two chosen polyhedra.

TABLE I. Cell constants (Å) for cotunnite-structured compounds at ambient pressure, space group $Pnam$, $Z = 4$.

	a	b	c	Ref.
PbCl ₂	7.6286(3)	9.0505(3)	4.5396(2)	This work ^a
BaCl ₂	7.871	9.430	4.730	11
BaBr ₂	8.252	9.915	4.935	11
SnCl ₂	7.793	9.207	4.43	12

^aAmbient cell data for PbCl₂ were obtained on a diffractometer using Cu $K\beta$ radiation. All figures in parentheses refer to standard deviations.

PbO₂ transforms in a series of transitions to the fluorite structure⁴ and then to the cotunnite structure.⁵ A significant number of other oxides and fluorides transform to this structure under pressure.⁶⁻⁸ The structure of the postcotunnite phase that we have obtained at high pressure for PbCl₂, BaCl₂, BaBr₂, and SnCl₂ is hence of great significance as the probable high-pressure structure type for a large and varied selection of compounds.

II. EXPERIMENTAL SECTION

Powdered PbCl₂, BaCl₂, BaBr₂, and SnCl₂ (Alfa Products) along with a ruby pressure calibrant were placed in 200- μ m-diam holes in inconel or stainless-steel gaskets preindented to a thickness of 100 μ m between the anvils of a diamond-anvil cell. The rear diamond was mounted over a wide slit permitting access to an angular range of $4\theta = 80^\circ$. Vacuum grease was used as a pressure-transmitting medium for the PbCl₂ experiment, whereas the other halides were loaded directly to prevent hydration. Pressures were measured based on the shift of the ruby R_1 fluorescence line.⁹ X-ray-diffraction patterns were obtained on films placed at a distance of 59.87 or 71.96 mm using zirconium-filtered molybdenum radiation from a fine-focus tube. Exposure times were of the order of 48 h. For some intermediate points on the compression curves, films were placed at 25.27 mm allowing a reduction in exposure time to 24 h. All experiments were performed at room temperature. Films were analyzed using a molecular-dynamics personal densitometer. Observed intensities were integrated as a function of 2θ , according to the method of Meade and Jeanloz.¹⁰

III. RESULTS AND DISCUSSION

Cotunnite-structured PbCl₂, BaCl₂, BaBr₂, and SnCl₂, Table I, were found to undergo phase transitions at 16, 9, 7.5, and 16 GPa, respectively, on compression. Previous work¹³ on BaCl₂ indicated the presence of a transition from the cotunnite phase; however, the structure of the

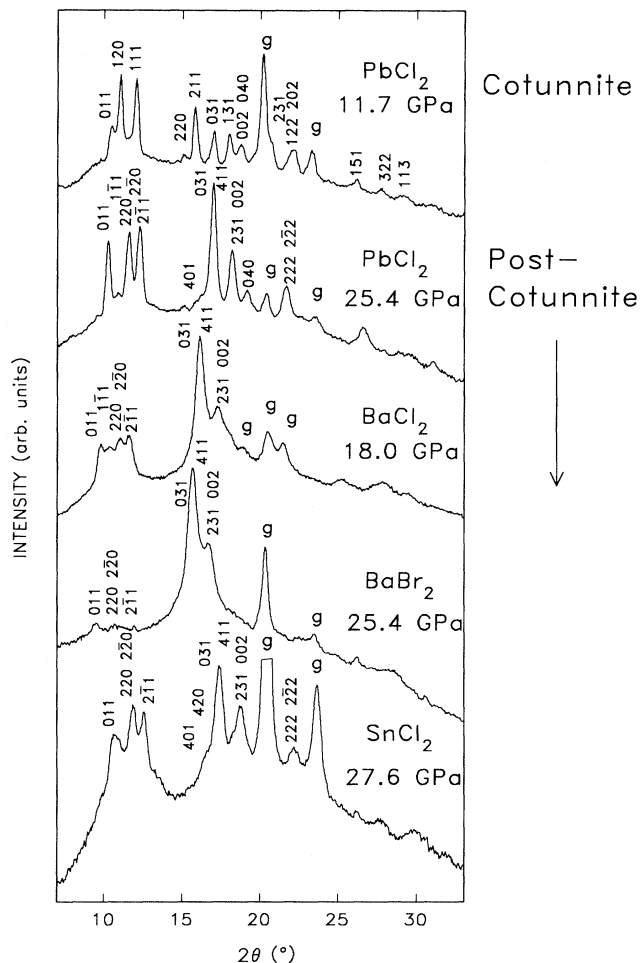


FIG. 2. X-ray-diffraction patterns of cotunnite PbCl₂ (above) and postcotunnite PbCl₂, BaCl₂, BaBr₂, and SnCl₂ (below). Reflections due to the gasket, stainless steel for BaCl₂ and inconel for the other compounds, are labeled g.

new phase was not determined. The high pressure transitions in these halides were reversible and exhibited a degree of hysteresis; in the case of PbCl₂, the reverse transition was found to begin at 7.3 GPa. At the transitions, new diffraction patterns were observed, Fig. 2; however, the peak intensities bore a resemblance to those in the parent cotunnite phase, indicating a possible relationship between the structures of the two phases. The diffraction patterns of the high-pressure phases were indexed based on a monoclinic cell with $Z = 8$, and refined cell constants are listed in Table II. Relationships between the cell constants of the low- and high-pressure phases are evident with a 2% and 4% increase in b and c , respective-

TABLE II. Cell constants (Å) for postcotunnite-structured compounds, space group $P112_1/a$, $Z = 8$.

	P (GPa)	a	b	c	γ (°)
PbCl ₂	25.4	11.995(10)	8.589(7)	4.491(3)	89.2(2)
BaCl ₂	18.1	12.511(13)	9.026(11)	4.704(3)	87.2(1)
BaBr ₂	25.4	12.773(14)	9.302(13)	4.896(4)	88.0(2)
SnCl ₂	27.7	11.856(30)	8.360(29)	4.331(9)	89.0(5)

ly, at the phase transition in the case of PbCl_2 . Superlattice peaks indicate a doubling of the unit cell relative to cotunnite along a . At 16 GPa, the cell constant $a/2$ of the high pressure phase is 11% shorter than the cotunnite a . The compression data for PbCl_2 , for which a volume decrease of $4.5 \pm 0.5\%$ was observed at the transition, are shown in Fig. 3.

Simulations of the powder diagrams performed with the program FULLPROF (Ref. 15) yielded the best results using the space group $P112_1/a$, which corresponds to the doubling of the cell with the $Pnam$ subgroup symmetry $P112_1/m$ along a . The scale factor, cell constants, overall thermal parameter, and linewidth parameters were refined using FULLPROF. Atomic positions beginning with those of cotunnite¹⁶ were adjusted in order to obtain the best agreement with the experimental profiles of the four halides investigated. In particular, the Pb-ion positions were first adjusted based on the PbCl_2 data, fol-

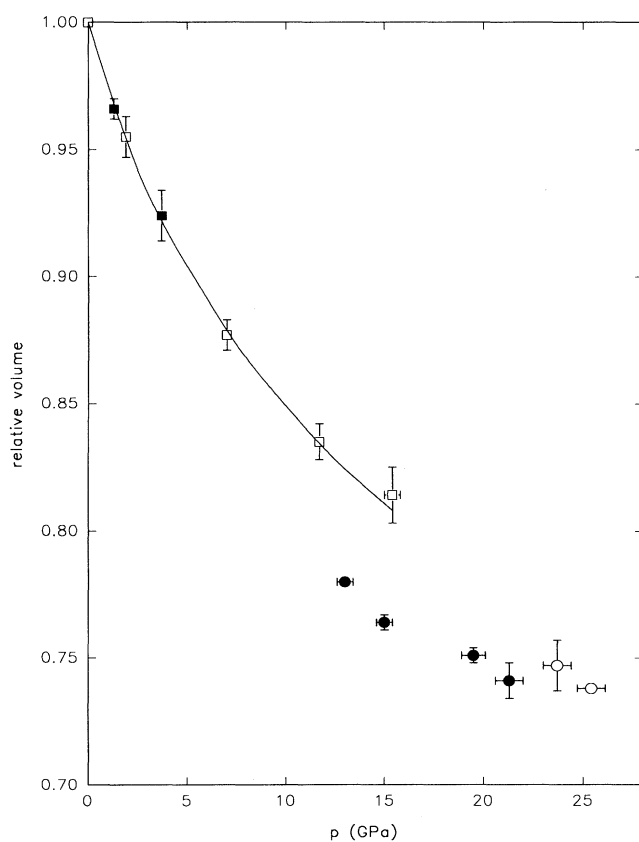


FIG. 3. Pressure-volume dependence of PbCl_2 . Open symbols refer to points obtained on compression and solid symbols to those obtained on decompression for the cotunnite (\square) and postcotunnite (\circ) phases. The solid line represents a Birch-Murnaghan equation of state (Ref. 14) fit of the cotunnite data with a bulk modulus at ambient pressure (B_0) of 34(1) GPa and $(\partial B/\partial p)_0 = 7.4(6)$. Horizontal and vertical error bars represent the uncertainty in pressure and the standard deviation in the relative volume, respectively. Additional points were obtained close to the transition; however, it was not possible to obtain reliable cell volumes due to peak overlap arising from the mixture of phases present.

TABLE III. Diffraction data for PbCl_2 at 25.4 GPa (only intense reflections are listed).

d (\AA)	I_{obs}	I_{cal}^a	hkl
3.980	96	76	011
3.770	4	2	$\bar{1}11$
3.513	68	54	220
3.465	66	64	$\bar{2}20$
3.326	22	18	211
3.306	99	86	$\bar{2}11$
2.494	8	10	401
2.474	6	6	420
2.441	30	36	$\bar{4}20$
2.413	78	82	031
2.402	100	100	411
2.248	46	46	231
2.246	54	54	002
2.229	16	16	$\bar{2}31$
2.145	22	20	040
1.893	30	26	222
1.885	36	30	$\bar{2}22$
1.868	28	28	$\bar{4}31$
1.781	18	24	611
1.653	18	24	$\bar{4}22$
1.551	20	18	042
1.548	20	16	631
1.543	30	24	$\bar{2}51$

^aAs calculated by FULLPROF.

lowing which these positions were taken as a starting point for the Ba ions for the BaCl_2 diagram, which was used for the adjustment of the chloride-ion positions. Final minor adjustments were made for each compound individually. Those positions that produced the best simulation for PbCl_2 , giving $\sum |I_{\text{obs}} - I_{\text{calc}}| / \sum I_{\text{obs}} = 11.8\%$, Fig. 4 and Table III, are listed in Table IV. The diagrams of the high-pressure phases of the other three halides can be simulated with similar agreement factors based on the same structure type with only minor modifications to these atomic positions. The diffraction patterns of these four AX_2 compounds, in which the ions have very different scattering factors, exhibit important variations in the relative intensities of the observed diffraction peaks; they can, nevertheless, be successfully simulated by the same structure type. In addition, comparison between the experimental and calculated diagrams over a large pressure range indicates that no significant changes in atomic positions occur as a function of pressure.

The resulting structural model for the postcotunnite phase, Fig. 1, consists of tetracapped trigonal prisms of

TABLE IV. Atomic positions used to simulate the diffraction pattern of PbCl_2 at 25.4 GPa.

	x	y	z
Pb(1)	0.167	0.124	0.266
Pb(2)	0.140	0.617	0.766
Cl(1)	0.110	0.458	0.280
Cl(2)	0.050	0.930	0.720
Cl(3)	0.007	0.270	0.720
Cl(4)	0.731	0.772	0.280

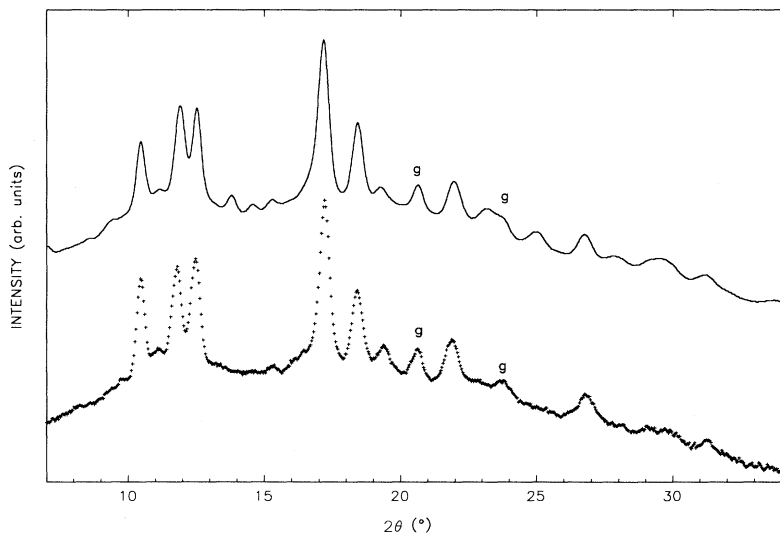


FIG. 4. Simulated (solid) and experimental (+) x-ray-diffraction patterns of postcotunnite PbCl_2 at 25 GPa. Reflections due to the gasket are labeled g. The background was fitted by interpolation between 17 points. The linewidths of the pseudo-Voigt functions used to fit the diffraction lines are defined as follows: $\text{FWHM}^2 = 14.2 \tan^2\theta - 2.6 \tan\theta + 0.25$ (where FWHM means full width at half maximum).

anions giving the cation a coordination number of 10. The 10 polyhedral cation-anion distances for PbCl_2 at 15 GPa range from 2.57 to 3.49 Å for Pb(1) and from 2.63 to 3.74 Å for Pb(2), as opposed to the nine that range from 2.66 to 3.41 Å in cotunnite at the same pressure assuming ambient atomic positions. The corresponding average Pb-Cl distances are 3.07 and 3.05 Å, respectively, for the two polyhedra in the postcotunnite phase and 2.92 Å in the cotunnite phase at 15 GPa. This increase in average Pb-Cl distance is what is expected to occur for an increase in CN from 9 to 10. The increase in the dispersion in the cation-anion distances is also not unusual as cations with different coordination numbers have been observed to exhibit significant differences in the range of distances to their coordinated anions, as in the case of the rare-earth disilicates.¹⁷

This new high-pressure structure is related to the Co_2Si -type structure, space group $Pn\bar{m}$, adopted by many covalent and intermetallic AB_2 compounds, in which the A atom is also in tenfold coordination. In fact, the cell constant ratios for the subcell of high pressure PbCl_2 , $a/c = 1.34$, and $b/c = 1.91$ are very close to those of Co_2Si ,¹⁸ $a/c = 1.32$, and $b/c = 1.90$. In contrast, the corresponding values for cotunnite under ambient conditions are 1.68 and 1.99, respectively. The main differences between the postcotunnite PbCl_2 structure and that of Co_2Si are that the unit cell of the former is monoclinic and doubled along the a direction as required

by the observed superlattice peaks. In addition, two distinct Pb centered polyhedra exist, one in which the Pb^{2+} ion lies on the same face and another in which it lies on a different face of the trigonal prism relative to that of a hypothetical Co_2Si -type PbCl_2 , Fig. 1. The cotunnite \rightarrow postcotunnite transition is first order and in symmetry terms can be envisaged as being comprised of two steps: a monoclinic distortion corresponding to the group-subgroup descent $Pn\bar{m} \rightarrow P112_1/m$ and a cell doubling step $P112_1/m \rightarrow P112_1/a$.

IV. CONCLUSION

The cotunnite \rightarrow postcotunnite phase transition corresponds to an increase in metal-ion coordination from 9 to 10 at the phase transition, which has not previously been observed in these ionic compounds. These halides are the first examples of ionic AX_2 compounds adopting a structure related to one up to the present only encountered among covalent and intermetallic compounds, which could indicate a tendency towards covalent or metallic bonding in these salts under high pressure. This new postcotunnite phase is of considerable importance for the crystal chemistry of the AX_2 compounds, as it is the probable high-pressure phase for many of the more than 400 compounds, which are known to adopt the cotunnite structure, and hence represents a new step in the phase transition sequence in these materials.

¹B. G. Hyde, M. O'Keeffe, W. M. Lyttle, and N. E. Brese, *Acta Chem. Scand.* **46**, 216 (1992).

²K. F. Seifert, *Fortschr. Miner.* **45**, 214 (1968).

³S. M. Stishov, *Dokl. Akad. Nauk. SSSR* **148**, 1186 (1963).

⁴Y. Syono and S. Akimoto, *Mater. Res. Bull.* **3**, 153 (1968).

⁵J. Haines, J. M. Léger, and A. Atouf (unpublished).

⁶L. Liu, *High Temp. High Pressure* **13**, 387 (1981).

⁷L. Merrill, *J. Phys. Chem. Ref. Data* **11**, 1005 (1982).

⁸S. J. Duclos, Y. K. Vohra, A. L. Ruoff, A. Jayaraman, and G. P. Espinosa, *Phys. Rev. B* **38**, 7755 (1988).

⁹H. K. Mao, P. M. Bell, J. W. Shaner, and D. J. Steinberg, *J. Appl. Phys.* **49**, 3276 (1978).

¹⁰C. Meade and R. Jeanloz, *Rev. Sci. Instrum.* **61**, 2571 (1990).

¹¹S. A. Hodorowicz, E. K. Hodorowicz, and H. A. Eick, *J. Solid State Chem.* **48**, 351 (1983).

¹²J. M. Van den Berg, *Acta Crystallogr.* **14**, 1002 (1961).

¹³J. M. Léger and A. Atouf, *J. Phys. Condens. Matter* **4**, 357 (1992).

¹⁴F. Birch, *Phys. Rev.* **71**, 809 (1947).

¹⁵J. Rodriguez-Carvajal (unpublished).

¹⁶K. Sahl and J. Zeeman, *Naturwissenschaften* **20**, 641 (1961).

¹⁷J. Felsche, in *Structure and Bonding*, edited by J. D. Dunitz *et al.* (Springer-Verlag, Berlin, 1973), Vol. 13, pp. 99–197.

¹⁸S. Geller, *Acta Crystallogr.* **8**, 83 (1955).